

# Watt-Hour Metering Characteristics at Scott Transformer in AC Electric Railway Systems

Hansang Lee\*, Kyebyung Lee\*\*, Kisuk Kim\*\*\*, Yong-Up Park§, Young-Soo Jeon§, Sung-Kwan Joo\*\*\*, Gilsoo Jang\*\*\*, Chang-Hyun Park†

**Abstract** – Owing to the consistent increase in accurate analysis issue for energy consumption of the AC electric railway systems, there is controversy about the adequacy of the present watt-hour metering configuration. Due to the unusual load characteristics and facilities, the discussions have not been active. Therefore, in order to achieve more accurate watt-hour metering for AC electric railway system, this paper proposes numerical formulas for watt-hour metering that reflects the highly-varying characteristics of the railway load and the structural characteristics of the Scott transformer. The proposed formulas have been verified by comparison with site-measured data, and a more suitable metering configuration for AC railway system has been proposed.

**Keywords:** AC electric railway system, Scott transformer, Scott connection, Regenerative power, Highly-varying load characteristics, Watt-hour metering.

## 1. Introduction

The AC electric railway system is one of the most representative and conventional electric transportation system. It is a massive transportation system with a primary purpose of transporting commuters or cargo, but in terms of electric energy network, it is one of the large capacity electrical loads. In the viewpoint of electric load, it is characterized by the position shift of electric load, intermittency of energy consumption, large regenerative power, and large-capacity single-phase load.

Since the railway system is designed for transportation, the movement of the load means that the electrical distance between the load and the source changes every moment. The change in electrical distance depends on the operation mode(dwelling-accelerating-coasting-braking) which is the main cause of the intermittency of energy consumption [1,2]. Especially, during braking mode, the electrical braking system applied for efficient braking converts the kinetic energy of the moving vehicle into electrical energy[3], which is re-supplied from the vehicle to the catenary system in the form of regenerative energy [4,5].

While the above three characteristics are simply physical phenomena based on the design purpose of the railway system, the fourth one is related to the reliability of the

operation. In order to achieve a high traction force, high-power three-phase induction motors are installed inside the vehicle, but it is difficult to reliably supply three-phase electric power by a wire contact method. For this reason, in spite of the high capacity of electrical load, it is adopted as a single-phase supply system. The equipment required to feed such large capacity of single-phase railway loads is a Scott transformer. The Scott transformer is a facility that supplies electric power from three phases to two single-phase, M and T phase [6,7]. The combination of the specificity of the Scott connection and the characteristics of the railway load of high intermittency and regenerative power presents very unusual results in terms of watt-hour metering. This paper proposes a suitable watt-hour metering configuration for AC railway system by derivation of the measured watt-hour value for arbitrary railway load(s) and verification for derived formula using the site-measured results. This paper is organized as follows. Chapter 2 presents the derivation of the voltage, current, and power relations at both ends of the Scott transformer. Chapter 3 describes the metering formulas for three types of metering configuration. Chapter 4 includes the verification of formulas by comparison with the site-measured data and case studies to choose suitable metering configuration.

## 2. V-I Relations between Primary and Secondary Windings of Scott Transformer

The Scott transformer is a transformer designed to convert the three-phase power into two single-phase by forming two connections between phase A and virtual neutral point, i.e electrical middle point of phase B and C, and between phase B and phase C as shown in Fig. 1 [8].

† Corresponding Author: Dept. of Electrical Engineering, Pukyong National University, Korea. (spch@pknu.ac.kr)

\* BK21+ Humanware IT Program, Korea University, Korea. (hansang80@korea.ac.kr)

\*\* Eco-friendly Transfer System Research Center, Pukyong National University, Korea. (kyebyung@pknu.ac.kr)

\*\*\* School of Electrical Engineering, Korea University, Korea. ({kks1213, skjoo, gjang}@korea.ac.kr)

§ Power Distribution Laboratory, KEPRI, Korea. ({yu.park, ys\_jeon}@kepco.co.kr)

Received: December 27, 2017; Accepted: February 2, 2018

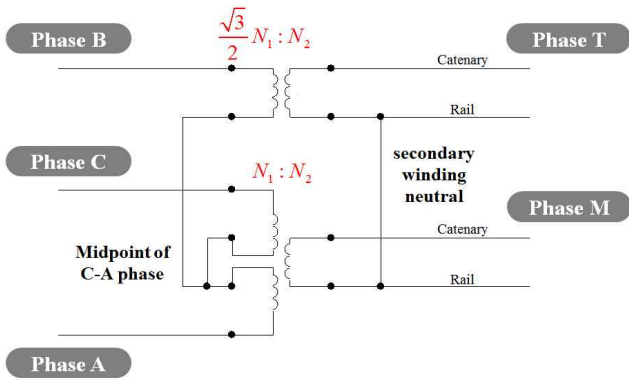


Fig. 1. Windings in scott transformer

From the perspective of the primary winding, the first and second winding appear as the phase voltage on phase A and the line-to-line voltage between B-C, respectively. In order to correct the conversion ratio from the phase voltage and the line voltage, turn ratio of each windings is set as shown in Fig 1.

When the phase B is set to the reference phase, the phase voltage and the line-to-line voltage for each phase of the primary side of the Scott transformer are expressed as Eq. (1)-(6).

$$v_a = V_{ph} \angle 2\pi / 3 \quad (1)$$

$$v_b = V_{ph} \angle 0 \quad (2)$$

$$v_c = V_{ph} \angle 4\pi / 3 \quad (3)$$

$$v_{ab} = \sqrt{3} \cdot V_{ph} \angle 5\pi / 6 \quad (4)$$

$$v_{bc} = \sqrt{3} \cdot V_{ph} \angle \pi / 6 \quad (5)$$

$$v_{ca} = \sqrt{3} \cdot V_{ph} \angle 3\pi / 2 \quad (6)$$

where,  $V_{ph}$  : nominal RMS voltage of phase voltage  
 $v_a, v_b, v_c$  : phase voltage RMS of primary side  
 $v_{ab}, v_{bc}, v_{ca}$  : line-to-line RMS voltage of primary side

The turn ratio of each winding of the Scott transformer is as shown in Eq. 7 and 8. Because the magnitude of the each primary voltage is different, it is designed to have different turns ratio to make the secondary voltage same level. Considering turn ratio of each winding, voltage of phase M and T in secondary winding are derived as Eq. (9) and (10). In Eq. (10), it should be noted that the voltage applied to the winding ration,  $n_T$ , is  $3/2v_b$ , since the primary voltage coupled to the phase T is the voltage between the midpoint on phase A-C and the phase B.

$$n_M = \frac{N_2}{N_1} = n \quad (7)$$

$$n_T = N_2 / \left( \frac{\sqrt{3}}{2} \cdot N_1 \right) = \frac{2}{\sqrt{3}} \cdot n \quad (8)$$

$$\begin{aligned} v_M &= n_M v_{ca} = n \cdot \left( \sqrt{3} V_{ph} \angle \frac{3\pi}{2} \right) \\ &= \sqrt{3} n V_{ph} \angle \frac{3\pi}{2} = V_{sw} \angle \frac{3\pi}{2} \end{aligned} \quad (9)$$

$$\begin{aligned} v_T &= n_T \cdot \left( \frac{3}{2} v_b \right) = \frac{2}{\sqrt{3}} n \cdot \left( \frac{3}{2} \cdot V_{ph} \angle 0 \right) \\ &= \sqrt{3} n V_{ph} \angle 0 = V_{sw} \angle 0 \end{aligned} \quad (10)$$

where,  $n_M, n_T$  : turn ratio of each winding  
 $N_1, N_2$  : turn of each winding  
 $v_M, v_T$  : phase voltage of secondary side  
 $V_{sw}$  : RMS phase voltage of secondary side

## 2.1 Load with power factor, $\cos \phi_M$ , at phase M

In order to derive the primary side current of the Scott Transformer, the M phase load current with power factor,  $\cos \phi_M$ , is assumed as shown in Eq. 11. Then, active and reactive power of M phase load are shown in Eq. 12.

$$i_M = I_M \angle \frac{3\pi}{2} - \phi_M \quad (11)$$

$$\begin{aligned} S_M &= P_M + jQ_M = v_M \cdot i_M^* \\ &= V_{sw} I_M \cos \phi_M + j V_{sw} I_M \sin \phi_M \\ &= \sqrt{3} n V_{ph} I_M \cos \phi_M + j \sqrt{3} n V_{ph} I_M \sin \phi_M \end{aligned} \quad (12)$$

where,  $i_M$  : M phase current  
 $I_M$  : M phase current RMS value  
 $\phi_M$  : phase angle difference for M phase load  
 $S_M, P_M, Q_M$ : apparent, active, and reactive power for M phase load

Since phase M is coupled only to the phase C and A, the phase currents on the primary side of Scott transformer are shown in Eq. (13)-(15).

$$i_{aM} = -n \cdot i_M = -n \cdot I_M \angle \frac{3\pi}{2} - \phi_M \quad (13)$$

$$i_{bM} = 0 \quad (14)$$

$$i_{cM} = n \cdot i_M = n \cdot I_M \angle \frac{3\pi}{2} - \phi_M \quad (15)$$

where,  $i_{aM}, i_{bM}, i_{cM}$  : primary side phase current induced by M phase load

## 2.2 Load with power factor, $\cos \phi_T$ , at phase T

In the same way as in the previous section, the T phase load current with power factor,  $\cos \phi_T$ , is assumed as shown in Eq. 16 and the active and reactive power of T phase load are shown in Eq. 17.

$$i_T = I_T \angle -\phi_T \quad (16)$$

$$\begin{aligned}
 S_T &= P_T + jQ_T = v_T \cdot i_T^* \\
 &= V_{sw} I_T \cos \phi_T + jV_{sw} I_T \sin \phi_T \\
 &= \sqrt{3} n V_{ph} I_T \cos \phi_T + j\sqrt{3} n V_{ph} I_T \sin \phi_T
 \end{aligned}
 \tag{17}$$

where,  $i_T$  : T phase current  
 $I_T$  : magnitude of T phase current  
 $\phi_T$  : phase angle difference for T phase load  
 $S_T, P_T, Q_T$ : apparent, active, and reactive power for T phase load

Since phase M is coupled only to the phase B and the midpoint is in the electrical middle point of phase A and C, the phase currents on the primary side of Scott transformer are shown in Eq. (18)-(20).

$$i_{aT} = -\frac{1}{2} i_{bT} = -\frac{1}{\sqrt{3}} n \cdot I_T \angle -\phi_T \tag{18}$$

$$i_{bT} = \frac{2}{\sqrt{3}} n \cdot i_T = \frac{2}{\sqrt{3}} n \cdot I_T \angle -\phi_T \tag{19}$$

$$i_{cT} = -\frac{1}{2} i_{bT} = -\frac{1}{\sqrt{3}} n \cdot I_T \angle -\phi_T \tag{20}$$

where,  $i_{aT}, i_{bT}, i_{cT}$ : primary side phase current induced by T phase load

### 2.3 Total phase current on primary side

From Eq. (13)-(15) and (18)-(20), the total phase current on primary side induced by M phase load and T phase load which are not unity power factor are derived as shown in Eq. (21)-(23).

$$\begin{aligned}
 i_a &= i_{aM} + i_{aT} \\
 &= \left( -n \cdot I_M \angle \frac{3\pi}{2} - \phi_M \right) + \left( -\frac{1}{\sqrt{3}} n \cdot I_T \angle -\phi_T \right)
 \end{aligned}
 \tag{21}$$

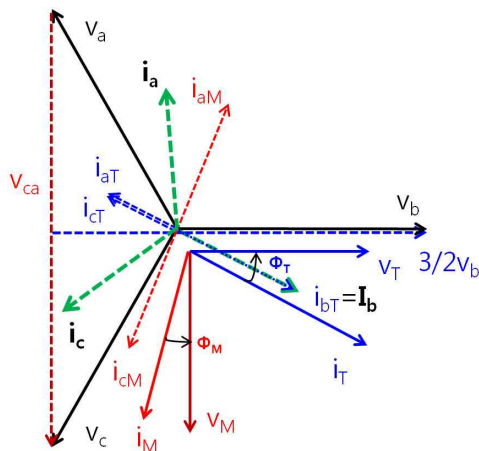


Fig. 2. Vector diagram for voltage and current between primary and secondary side of Scott transformer

$$i_b = i_{bM} + i_{bT} = 0 + \frac{2}{\sqrt{3}} n \cdot I_T \angle -\phi_T \tag{22}$$

$$\begin{aligned}
 i_c &= i_{cM} + i_{cT} \\
 &= \left( n \cdot I_M \angle \frac{3\pi}{2} - \phi_M \right) + \left( -\frac{1}{\sqrt{3}} n \cdot I_T \angle -\phi_T \right)
 \end{aligned}
 \tag{23}$$

The vector diagram of voltage-current relationship between the primary and secondary side of the Scott transformer is illustrated in Fig. 2.

## 3. Electrical Energy Metering for AC Electric Railway Systems

The metering of the consumed energy for the AC railway system takes place on the primary side of the Scott transformer. Watt-hour metering for the three-phase system generally applies 2-CT metering for 3-phase 4-wire systems or 3-CT metering for 3-phase 3-wire systems. Although the AC electric railway system consists of 3-phase 3-wire system, the metering formula for each metering system is derived as follows based on the formula derived from Chapter 2 in order to compare with the result obtained through actual measurement. It is assumed that the electrical loads on phase M and phase T are as in Eq. (12) and (17).

### 3.1 3-CT metering system

Generally, the 3-CT metering is a method of measuring the amount watt-hour of each phase by using the phase current and voltage between phase voltage and neutral line voltage as shown in Fig. 3. For each time step, the amount of watt-hour accumulated in meter at each phase are derived by Eq. (24)-(26).

When the unity power factor loads are taken into consideration for M phase and T phase respectively, it is well known that the M phase and T phase load are distributed to the primary side with 1:0:1 and 1:4:1 respectively. However, in the case of non-unity power

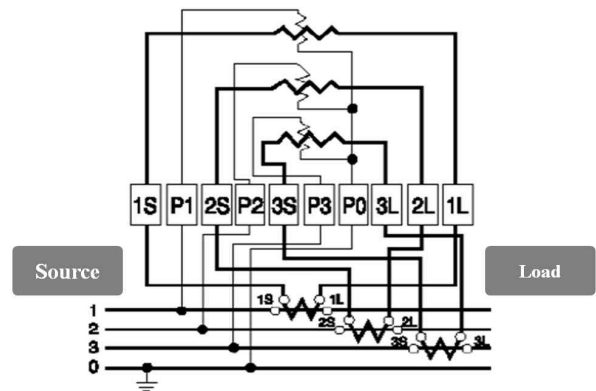


Fig. 3. 3-CT watt-hour meter connection

factor load the results of the watt-hour metering on the other two phases that are not coupled to the T phase are affected by the reactive power of each load as shown in Eq. (24) and (26). Although there is distortion in the metering results at each watt-hour meter, Eq. (27) shows that the instantaneous numerical sum is equal to the sum of the loads at secondary side.

$$\begin{aligned}
 E_a &= P_a \cdot \Delta t = \text{Re}[v_a \cdot i_a^*] \cdot \Delta t \\
 &= \text{Re} \left[ \left( V_{ph} \angle \frac{2\pi}{3} \right) \cdot \left( -n \cdot I_M \angle \frac{\pi}{2} + \phi_M - \frac{1}{\sqrt{3}} n \cdot I_T \angle \phi_T \right) \right] \cdot \Delta t \\
 &= \text{Re} \left[ nV_{ph} I_M \angle \frac{\pi}{6} + \phi_M \right] \cdot \Delta t + \text{Re} \left[ \frac{nV_{ph} I_T}{\sqrt{3}} \angle \frac{5\pi}{3} + \phi_T \right] \cdot \Delta t \\
 &= \left( \frac{\sqrt{3}}{2} nV_{ph} I_M \cos \phi_M - \frac{1}{2} nV_{ph} I_M \sin \phi_M \right) \cdot \Delta t \\
 &\quad + \left( \frac{\sqrt{3}}{6} nV_{ph} I_T \cos \phi_T + \frac{1}{2} nV_{ph} I_T \sin \phi_T \right) \cdot \Delta t \\
 &= \left( \frac{1}{2} P_M + \frac{1}{6} P_T + \frac{\sqrt{3}}{6} (-Q_M + Q_T) \right) \cdot \Delta t
 \end{aligned} \tag{24}$$

$$\begin{aligned}
 E_b &= P_b \cdot \Delta t = \text{Re}[v_b \cdot i_b^*] \cdot \Delta t \\
 &= \text{Re} \left[ \left( V_{ph} \angle 0 \right) \cdot \left( \frac{2}{\sqrt{3}} n \cdot I_T \angle \phi_T \right) \right] \cdot \Delta t \\
 &= \left( \frac{2\sqrt{3}}{3} nV_{ph} I_T \cos \phi_T \right) \cdot \Delta t \\
 &= \frac{2}{3} P_T \cdot \Delta t
 \end{aligned} \tag{25}$$

$$\begin{aligned}
 E_c &= P_c \cdot \Delta t = \text{Re}[v_c \cdot i_c^*] \cdot \Delta t \\
 &= \text{Re} \left[ \left( V_{ph} \angle \frac{4\pi}{3} \right) \cdot \left( n \cdot I_M \angle \frac{\pi}{2} + \phi_M - \frac{1}{\sqrt{3}} n \cdot I_T \angle \phi_T \right) \right] \cdot \Delta t \\
 &= \text{Re} \left[ nV_{ph} I_M \angle -\frac{\pi}{6} + \phi_M \right] \cdot \Delta t + \text{Re} \left[ \frac{nV_{ph} I_T}{\sqrt{3}} \angle \frac{\pi}{3} + \phi_T \right] \cdot \Delta t \\
 &= \left( \frac{\sqrt{3}}{2} nV_{ph} I_M \cos \phi_M + \frac{1}{2} nV_{ph} I_M \sin \phi_M \right) \cdot \Delta t \\
 &\quad + \left( \frac{\sqrt{3}}{6} nV_{ph} I_T \cos \phi_T - \frac{1}{2} nV_{ph} I_T \sin \phi_T \right) \cdot \Delta t \\
 &= \left( \frac{1}{2} P_M + \frac{1}{6} P_T + \frac{\sqrt{3}}{6} (Q_M - Q_T) \right) \cdot \Delta t
 \end{aligned} \tag{26}$$

$$\begin{aligned}
 P_{total\_3CT} &= \text{Re}[v_a \cdot i_a^*] + \text{Re}[v_b \cdot i_b^*] + \text{Re}[v_c \cdot i_c^*] \\
 &= P_M + P_T
 \end{aligned} \tag{27}$$

### 3.2 2-CT metering system with reference phase coupled to the T phase

The 2-CT metering system performs watt-hour metering using the phase currents of phases except for the reference

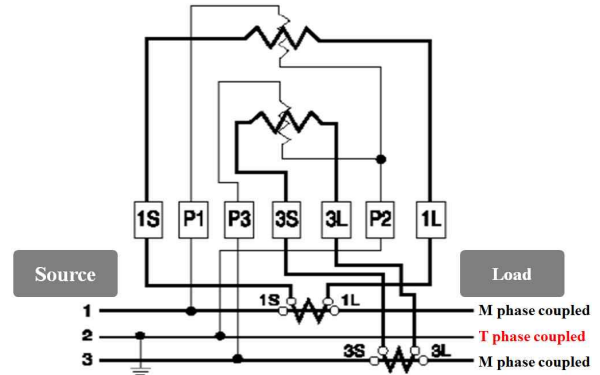


Fig. 4. 2-CT watt-hour meter connection with reference phase coupled to the T phase

phase and the line-to-line voltage from the reference phase as shown in Fig. 4. For each time step, the amount of accumulated watt-hour in each meter is derived by Eq. (28)-(29).

$$\begin{aligned}
 E_{ab} &= P_{ab} \cdot \Delta t = \text{Re}[v_{ab} \cdot i_a^*] \cdot \Delta t \\
 &= \text{Re} \left[ \left( \sqrt{3} \cdot V_{ph} \angle \frac{5\pi}{6} \right) \cdot \left( -n \cdot I_M \angle \frac{\pi}{2} + \phi_M - \frac{1}{\sqrt{3}} n \cdot I_T \angle \phi_T \right) \right] \cdot \Delta t \\
 &= \text{Re} \left[ \sqrt{3} nV_{ph} I_M \angle \frac{\pi}{3} + \phi_M \right] \cdot \Delta t + \text{Re} \left[ nV_{ph} I_T \angle -\frac{\pi}{6} + \phi_T \right] \cdot \Delta t \\
 &= \left( \frac{\sqrt{3}}{2} nV_{ph} I_M \cos \phi_M - \frac{3}{2} nV_{ph} I_M \sin \phi_M \right) \cdot \Delta t \\
 &\quad + \left( \frac{\sqrt{3}}{2} nV_{ph} I_T \cos \phi_T + \frac{1}{2} nV_{ph} I_T \sin \phi_T \right) \cdot \Delta t \\
 &= \left( \frac{1}{2} P_M + \frac{1}{2} P_T + \frac{\sqrt{3}}{6} (-3Q_M + Q_T) \right) \cdot \Delta t
 \end{aligned} \tag{28}$$

$$\begin{aligned}
 E_{cb} &= P_{cb} \cdot \Delta t = \text{Re}[v_{cb} \cdot i_c^*] \cdot \Delta t \\
 &= \text{Re} \left[ \left( \sqrt{3} \cdot V_{ph} \angle \frac{7\pi}{6} \right) \cdot \left( n \cdot I_M \angle \frac{\pi}{2} + \phi_M - \frac{1}{\sqrt{3}} n \cdot I_T \angle \phi_T \right) \right] \cdot \Delta t \\
 &= \text{Re} \left[ \sqrt{3} nV_{ph} I_M \angle -\frac{\pi}{3} + \phi_M \right] \cdot \Delta t + \text{Re} \left[ nV_{ph} I_T \angle \frac{\pi}{6} + \phi_T \right] \cdot \Delta t \\
 &= \left( \frac{\sqrt{3}}{2} nV_{ph} I_M \cos \phi_M + \frac{3}{2} nV_{ph} I_M \sin \phi_M \right) \cdot \Delta t \\
 &\quad + \left( \frac{\sqrt{3}}{2} nV_{ph} I_T \cos \phi_T - \frac{1}{2} nV_{ph} I_T \sin \phi_T \right) \cdot \Delta t \\
 &= \left( \frac{1}{2} P_M + \frac{1}{2} P_T + \frac{\sqrt{3}}{6} (3Q_M - Q_T) \right) \cdot \Delta t
 \end{aligned} \tag{29}$$

$$\begin{aligned}
 P_{total\_2CTb} &= \text{Re}[v_{ab} \cdot i_a^*] + \text{Re}[v_{cb} \cdot i_c^*] \\
 &= P_M + P_T
 \end{aligned} \tag{30}$$

Assuming unity power factor loads as phase M and T, Eq. (28) and (29) show that each watt-hour meter measures and

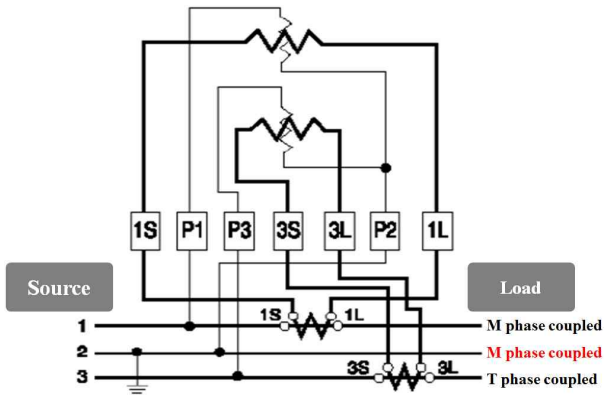


Fig. 5. 2-CT watt-hour meter connection with reference phase coupled to the M phase

accumulates half of the active power of each phase. However, as with the 3-CT method, when considering the load rather than the unit power factor, each watt-hour meter derives distorted results according to the reactive power of the two loads. In addition, since the railway load during braking has regenerative load as large as the consuming operation, the regenerative operation of one load might cause a large metering error.

### 3.3 2-CT metering system with reference phase coupled to the M phase

Unlike in Section 3.2, the 2-CT metering system is applied by setting the phase coupled with M phase as a reference phase. Then, Eq. (31) and (32) shows the amount of accumulated watt-hour in each meter.

$$\begin{aligned}
 E_{ba} &= P_{ba} \cdot \Delta t = \text{Re} [v_{ba} \cdot i_b^*] \cdot \Delta t \\
 &= \text{Re} \left[ \left( \sqrt{3} \cdot V_{ph} \angle -\frac{\pi}{6} \right) \cdot \left( \frac{2}{\sqrt{3}} n \cdot I_T \angle \phi_T \right) \right] \cdot \Delta t \\
 &= \left( \sqrt{3} n V_{ph} I_T \cos \phi_T + n V_{ph} I_T \sin \phi_T \right) \cdot \Delta t \\
 &= \left( P_T + \frac{1}{\sqrt{3}} Q_T \right) \cdot \Delta t
 \end{aligned} \tag{31}$$

$$\begin{aligned}
 E_{ca} &= P_{ca} \cdot \Delta t = \text{Re} [v_{ca} \cdot i_c^*] \cdot \Delta t \\
 &= \text{Re} \left[ \left( \sqrt{3} V_{ph} \angle \frac{3\pi}{2} \right) \cdot \left( n I_M \angle \frac{\pi}{2} + \phi_M - \frac{1}{\sqrt{3}} n I_T \angle \phi_T \right) \right] \cdot \Delta t \\
 &= \text{Re} \left[ \sqrt{3} n V_{ph} I_M \angle \phi_M \right] \cdot \Delta t + \text{Re} \left[ n V_{ph} I_T \angle \frac{\pi}{2} + \phi_T \right] \cdot \Delta t \\
 &= \left( P_M - \frac{1}{\sqrt{3}} Q_T \right) \cdot \Delta t
 \end{aligned} \tag{32}$$

$$P_{total\_2CTa} = \text{Re} [v_{ba} \cdot i_b^*] + \text{Re} [v_{ca} \cdot i_c^*] = P_M + P_T \tag{33}$$

Assuming unity power factor loads as phase M and T, Eq. (31) and (32) show that each watt-hour meter measures and accumulates active power of each phase. It should be noted

that the metering interference due to the regenerative operation of one load has been eliminated. However, any portion of the reactive power of the Q phase load still affects the metering.

## 4. Measured Data Verification and Case Studies

In order to verify whether the watt-hour metering result at the metering point is distorted when the railway vehicle is operating on the secondary side of the Scott transformer, real site measurement had been performed for the Scott transformer installed in the railway substation. Using measurement equipment which can measure with five time-

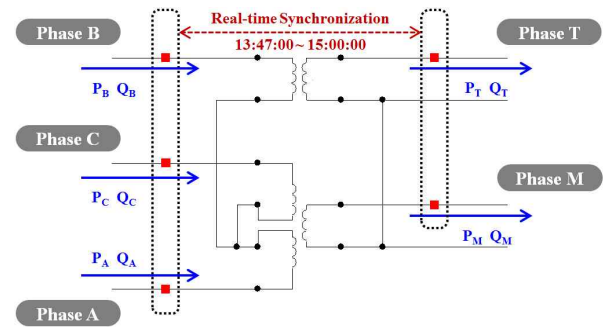


Fig. 6. Measurement for primary and secondary side of Scott Tr

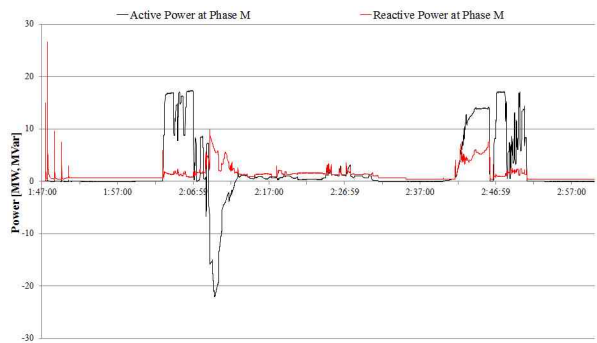


Fig. 7. Site measured active and reactive power for phase M load

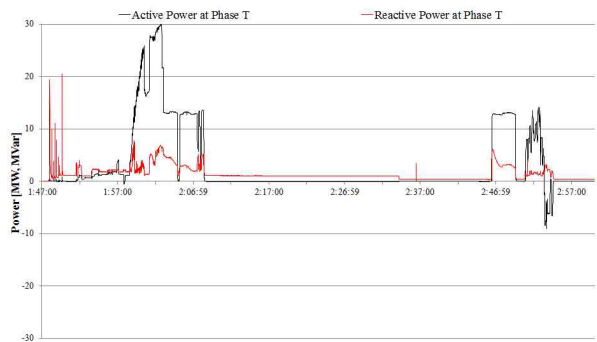


Fig. 8. Site measured active and reactive power for phase T load

synchronized channels, voltage and current measurement at the 5 measuring points in Fig. 6 had been performed.

#### 4.1 Measured data in AC railway substation

The power measuring results are shown in Fig. 7 and 8. The M-phase load consumes a maximum of 17.34 MW and has a maximum regenerative power of 22.06 MW during the regenerative operating. The T-phase load has a peak of 29.98 MW and a maximum regenerative power of 9.06 MW. Especially at the beginning of the measurement, it is necessary to pay attention to the high reactive power in both phases and how this affects the watt-hour metering.

Measurements were made on the A, B, and C phase on the primary side of Scott transformer. Figs. 9, 10, and 11 compare the simultaneously measured results of 3 phases on the primary side and the calculation results using Eq. (24)-(26) based on the measured results of Fig. 8 and 9.

As shown in Fig. 9, 10, and 11, the site-measured results and the numerical results are quite consistent. Especially, as proven in Eq. (25) that the accumulated energy at the B phase is independent of the reactive power of the M and T phase load(s), Fig. 10 shows that the active power measurement result on phase B is not affected for the high

reactive power at the beginning of the measurement. This also coincides with the numerical result.

Although the effective power of the two loads was close to zero at the beginning of the measurement, the actual power measurement results on A and C phase were measured to have significant values. As proven in Eq. (24) and (26), this is a result of the reactive power difference of the two loads and this might cause significant errors in the watt-hour metering.

#### 4.2 2-CT metering system with reference phase coupled to the T phase

Based on the Eq. (28) and (29), the numerical results of the active power at each meter for the 2-CT metering system with setting phase coupled T phase as a reference phase are illustrated in Fig. 12 and 13. They show that the each numerical result does not reflect actual measured values at all. That is, even if the 2-CT method should be applied due to the three-phase three-wire feeding structure, all of these results show that to set the phase coupled to the T phase as a reference phase might result in a significantly distorted metering results.

#### 4.3 2-CT metering system with reference phase coupled to the M phase

Using the Eq. (31) and (32), the numerical results of the

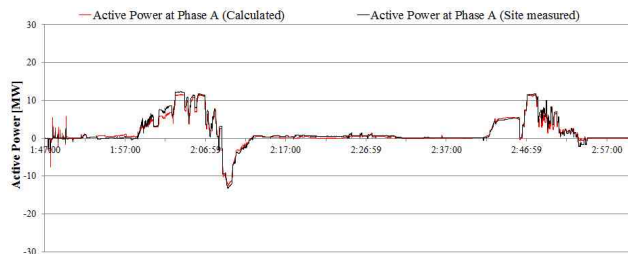


Fig. 9. Measured and calculated active power for phase A

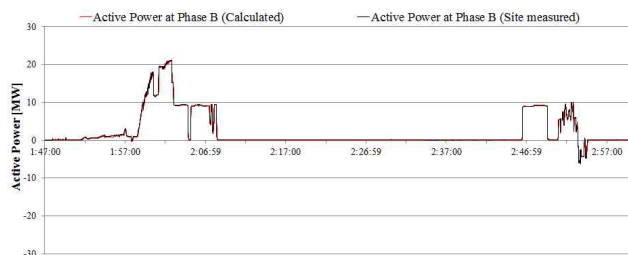


Fig. 10. Measured and calculated active power for phase B

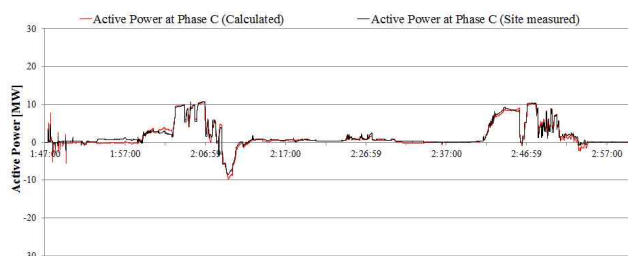


Fig. 11. Measured and calculated active power for phase C

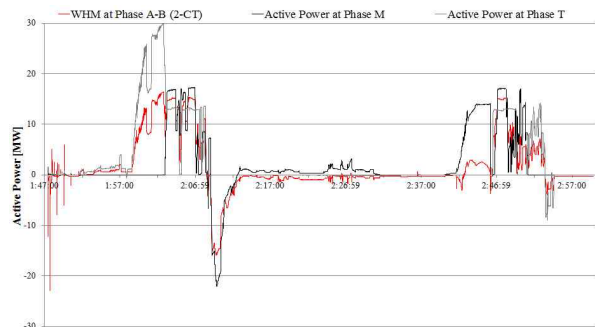


Fig. 12. Measurement at phase AB with M and T phase loads

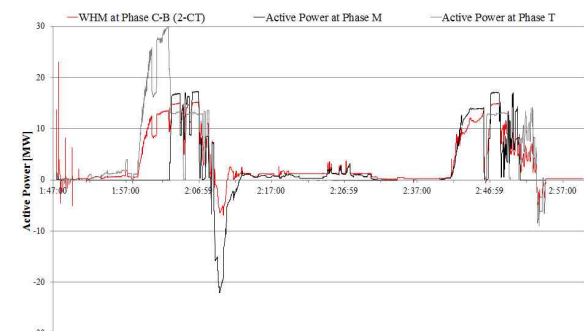


Fig. 13. Measurement at phase CB with M and T phase loads

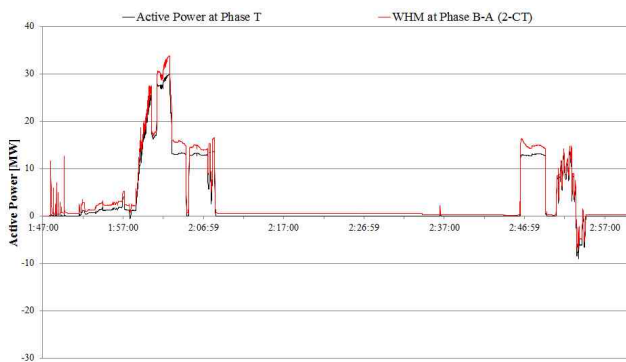


Fig. 14. Watt-hour metering results at phase BA and active power comparison with T phase load



Fig. 15. Watt-hour metering results at phase CA and active power comparison with M phase load

active power at each meter for the 2-CT metering system with setting phase coupled M phase as a reference phase are illustrated in Fig. 14 and 15. These show that the numerical results are considerably in agreement with the measured active power at each of the secondary sides of the Scott transformer.

## 5. Conclusion

This paper presents a numerical analysis of watt-hour metering characteristics at both ends of a Scott transformer by highly-varying operation of an AC railway load. In order to choose the appropriate watt-hour metering configuration, the analysis steps and the conclusions at each step are as follows:

- 1) Derivation of voltage, current, and power relations across the Scott transformer: Considering the characteristics of the Scott winding, the magnitude and phase of the secondary voltage under the balanced primary voltage condition are derived. Assuming an arbitrary power factor, the phase angle of the secondary current is defined and the primary side phase currents induced by the load current of each secondary phase are derived. Based on this, the power relations at both ends of the Scott

transformer are derived.

- 2) Derivation of metering formulas for each watt-hour metering configuration: For 3-CT, and two 2-CT metering configuration, the metering formulas that each meter will experience at each time step are derived. These formulas proved that the amount of accumulated energy is related to not only the active power but also the reactive power of the railway load at secondary side.
- 3) Verification of formulas for 3-CT configuration based on site-measured data: Based on the simultaneously measured data for the primary and secondary phases, the validity of the derived formulas was verified by comparing the numerical results with the site-measured results. It is proved that the reactive power of the load can be reflected as the active power to the each meter.
- 4) Choosing the suitable 2-CT configuration for railway system with Scott transformer: By comparing the numerical results based on the derived formulas with the measured results for each phase load, suitable metering configuration that better reflects the power characteristics of highly-varying railway loads has been chosen. Since each meter can measure and accumulate the M phase and T phase loads separately, the 2-CT method, which sets the phase coupled to the M phase as a reference phase, presents small metering distortion.

Based on this study on the energy metering in the AC railway system, rational diagnosis for electrical energy consumed by AC railway system is possible through accurate watt-hour metering and peak power calculation without metering distortion. Also in consideration of additional facilities or operational strategies for improving energy efficiency and energy sustainability, this precise metering can be an essential basis.

## Acknowledgements

This work was supported under the framework of international cooperation program managed by National Research Foundation of Korea (No. 2017K1A4A3013579).

This work was supported by the National Research Foundation of Korea (NRF) grant funded by the Korea government (MSIP) (No. NRF-2017R1A2B2004259).

## References

- [1] D. RajaPrivanka, G. ShanmugaPriya, R. Sabashini, V. M. E. Janintha, "Power generation and energy management in railway system," presented at the 3rd Int. Conf. on Science Technology Engineering & Management, Chennai, India, 2017.
- [2] V. T. Cheremisin, A. A. Komyakov, V. V. Erbes, "Simulation of power consumption in railway power

supply systems with of artificial intelligence aids,” presented at the Int. Conf. on Industrial Engineering, Applications and Manufacturing, St. Petersburg, Russia, 2017.

- [3] Mehran Shafiqhy, Sui Yang Khoo, Abbas Z. Kouzani, “Modified DSC Propulsion Systems for Efficient Direct Recovery of Regeneration in 25-kV AC Traction Power Supply,” *IEEE Trans. on Transp. Elect.*, vol. 3, Issue 3, pp. 632-645, Mar. 2017.
- [4] Hansang Lee, Hanmin Lee, Changmu Lee, Gilsoo Jang, Gildong Kim, “Energy Storage Application Strategy on DC Electric Railroad System using a Novel Railroad Analysis Algorithm,” *J. Electr. Eng. Technol.*, vol. 5, no. 2, pp. 228-238, Jun. 2010.
- [5] Hansang Lee, Seungmin Jung, Yoonsung Cho, Donghee Yoon, Gilsoo Jang, “Peak power reduction and energy efficiency improvement with the superconducting flywheel energy storage in electric railway system,” *Physica C*, vol. 494, pp. 246-249, Nov. 2013.
- [6] Changmu Lee, Hansang Lee, Dong-Hee Yoon, Hanmin Lee, Jiyoung Song, Gilsoo Jang, Byungmoon Han, “A Novel Fault Location Scheme on Korean Electric Railway System Using the 9-Conductor Representation,” *J. Electr. Eng. Technol.*, vol. 5, no. 2, pp. 220-227, Jun. 2010.
- [7] Yun Li, Peter A. Crossley, “Voltage balancing in low-voltage radial feeders using Scott transformers,” *IET Gener. Transm. Distrib.*, Vol. 8, Issue 8, pp. 1489-1498, Aug. 2014.
- [8] S.-H. Chang, K.-H. Oh, and J.-H Kim, “Analysis of voltage unbalance in the electric railway system using two-port network model,” *KIEE Trans.*, Vol. 50A, no. 5, pp. 248-254, May 2001.



**Hansang Lee** He received the Ph. D. degree in Electrical Engineering from Korea University, Seoul, Korea in 2010. He is presently a Research Professor of BK21+ Humanware IT Program at Korea University.



**Kyebuyng Lee** He received the B.S. and M.S. degrees from Dong-Eui University, Busan, Korea, in 2006 and 2008, respectively, and the Ph.D. degree in electrical engineering from Korea University, Seoul, Korea, in 2018. Currently, he is a Research Fellow with Pukyong National University, Busan, Korea. His research interests include power quality and power system control.



**Kisuk Kim** He received the B.S. Degree in electrical engineering from Soong-sil University, Seoul, Korea in 2010 and the M.S. degree from Korea University, Seoul, Korea in 2013. He is currently pursuing a Ph.D. degree at Korea University. His research interests are electric railway systems and real-time simulation for power systems.



**Yong Up Park** He received master’s degree in Electrical Engineering from Kangwon National University, Korea. He is presently a senior researcher of Smart distribution power system Lab. at KEPRI.



**Young Soo Jeon** He received master’s degree in Electrical Engineering from Chungnam National University, Korea. He is presently an Principal researcher of Smart distribution power system Lab. at KEPRI.



**Sung-Kwan Joo** He received the M.S. and Ph.D. degrees from the University of Washington, Seattle, in 1997 and 2004, respectively. He is currently a Professor in the school of electrical engineering at Korea University, Seoul, Korea.



**Gilsoo Jang** He received the B.S. and M.S. degrees in electrical engineering from Korea University, Seoul, Korea, in 1991 and 1994, respectively, and the Ph.D. degree in electrical and computer engineering from Iowa State University, Ames, in 1997. He was a Visiting Scientist at Iowa State University from 1997 to 1998 and a Senior Researcher with the Korea Electric Power Research Institute, Daejeon, Korea, from 1998 to 2000. Currently, he is a Professor in the School of Electrical Engineering, Korea University. His research interests include power quality and power system control.



**Chang-Hyun Park** He received the B.S. degree from Inha University, Incheon, Korea, in 2001, and the Ph.D. degree from Korea University, Seoul, Korea, in 2007. Currently, he is a Professor in the Department of Electrical Engineering at Pukyong National University. His research interests include

power quality assessment, data visualization, and computer simulation of power systems.